Flow around Clark-Y airfoil: Summary of EFD benchmark data and comparison with IIHR EFD data and CFD solution

Nobuaki Sakamoto, J. Colin Johnson, Stuart Breczinski, Marian V. Muste and Frederick Stern
IIHR-Hydroscience&Engineering, The University of Iowa

1. EFD benchmark data

[1] JACOBS E.N., STACK J., AND PINKERTON R.M., 1930 Airfoil pressure distribution investigation in the variable density wind tunnel, Langley Memorial Aeronautical Laboratory Report No. 353

[2] MARCHMAN J.F. AND WERME T.D., 1984 Clark-Y airfoil performance at low Reynolds numbers, In: proc. AIAA 22nd Aerospace Science Meeting, Jan. 9-12, Reno, Nevada, U.S.A.

[3] SILVERSTEN A., 1934, Scale effect on Clark-Y airfoil characteristics from NACA full-scale wind-tunnel tests, Langley Memorial Aeronautical Laboratory Report No. 502

[4] ZIMMERMAN C.H., Characteristics of Clark-Y airfoils of small aspect ratios, 1932, Langley Memorial Aeronautical Laboratory Report No. 431

The summary of EFD benchmark data is given in Table 1.

Table 1 Summary of EFD benchmark data

<table>
<tr><td>Reference</td><td>[1]</td><td colspan="2">[2]</td><td>[3]</td><td>[4]</td></tr>
<tr><td>Digitized data</td><td>C_p and C_L</td><td colspan="2">C_p, C_L and C_D</td><td>C_L and C_D</td><td>C_L and C_D</td></tr>
<tr><td>AR*</td><td>7.2</td><td colspan="2">5.75</td><td>6</td><td>0.5, 0.75, 1, 1.25, 1.5, 2, 3, 6</td></tr>
<tr><td rowspan="2">Re**</td><td rowspan="2">3.56e5</td><td>C_P</td><td>7.5e4</td><td rowspan="2">1.12e6, 1.55e6, 2.06e6, 2.81e6, 3.19e6, 3.59e6</td><td rowspan="2">8.6e5</td></tr>
<tr><td>C_L, C_D</td><td>5e4, 7.5e4, 1e5, 2e5, 6.7e6</td></tr>
<tr><td rowspan="2">α (deg)***</td><td rowspan="2">1, 4, 7, 10,13, 17, 20</td><td>C_P</td><td>0, 4, 6, 8, 12, 14</td><td rowspan="2">0, 1, 2, 3, 4, 5, 6, 7, 8, 9, 10, 11, 12, 13, 14, 15, 16, 17, 18, 19, 20, 21, 22, 23</td><td rowspan="2">0, 10, 15, 20, 25, 30, 35, 39, 40, 42, 50, 60</td></tr>
<tr><td>C_L, C_D</td><td>0, 4, 6, 8, 12, 14</td></tr>
<tr><td>Wingtip</td><td></td><td colspan="2">End plates</td><td>Wing cross section</td><td>Rectangular</td></tr>
</table>

*: Aspect ratio, **: Reynolds number, ***: Angle of attack

2. Trend of each data set

2.1 Reference [1]

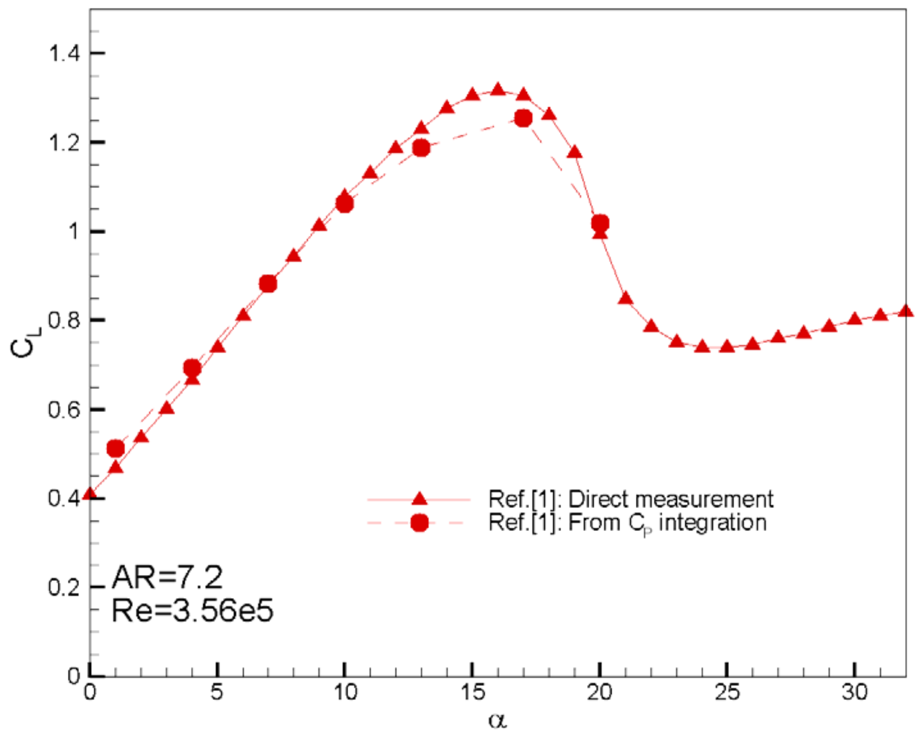

Fig. 1 Trend of C_L in Reference [1]

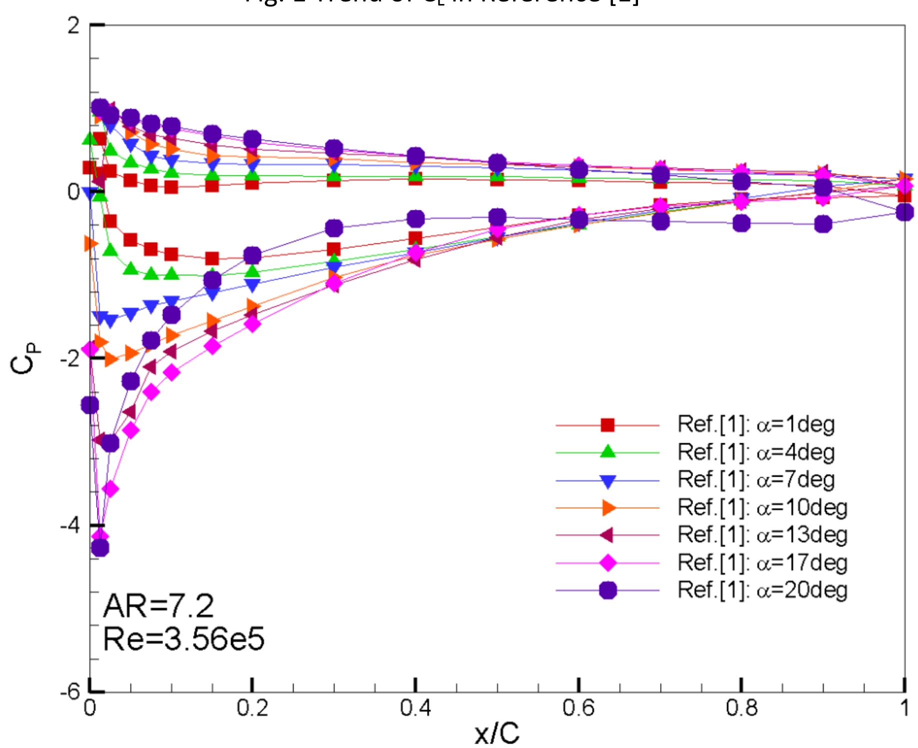

Fig. 2 Trend of C_P in Reference [1]

2.2 Reference [2]

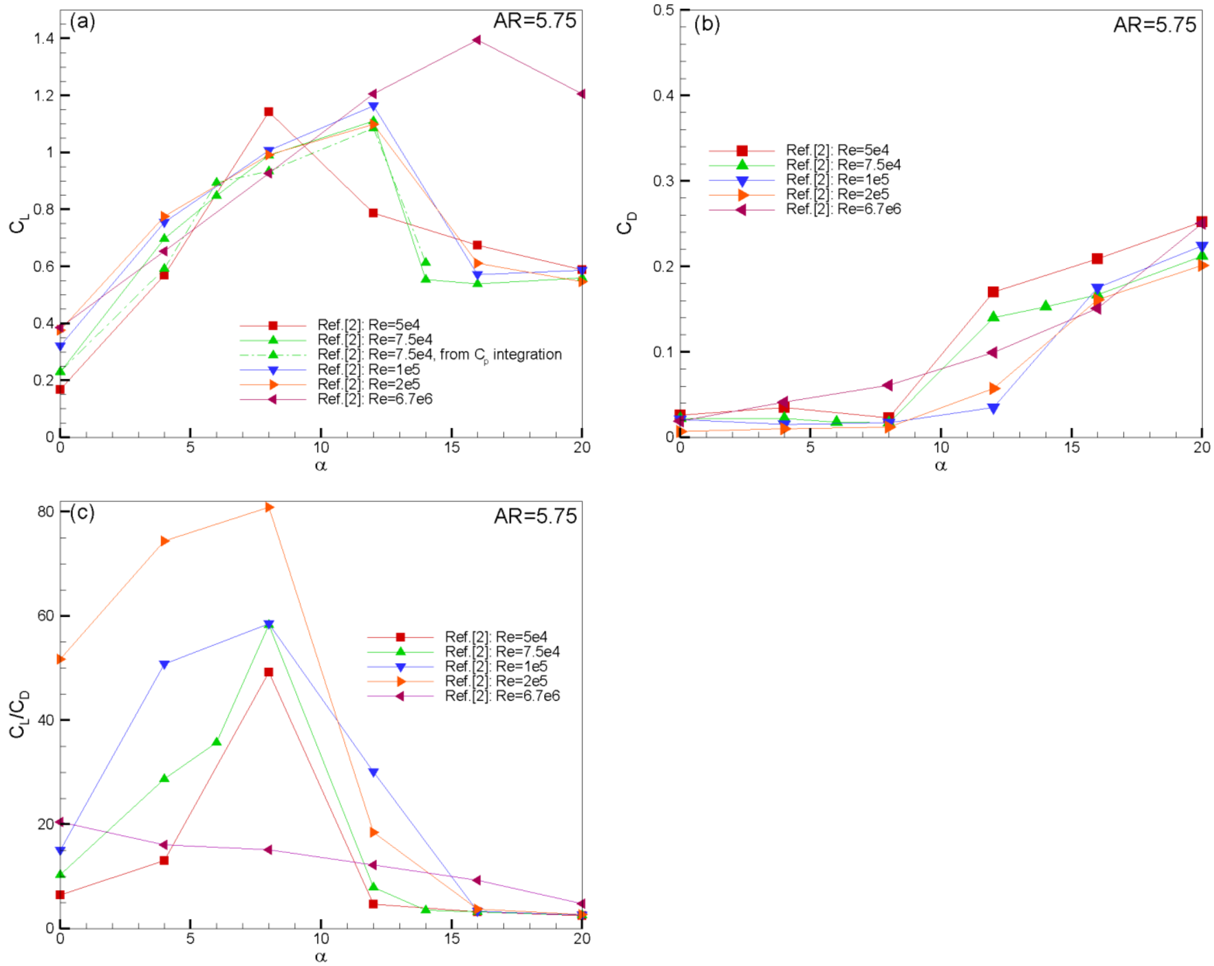

Fig. 3 Trend of C_L, C_D, and C_L/C_D with variations of Re in Reference [2]
(a) C_L vs α, (b) C_D vs α, (c) C_L/C_D vs α

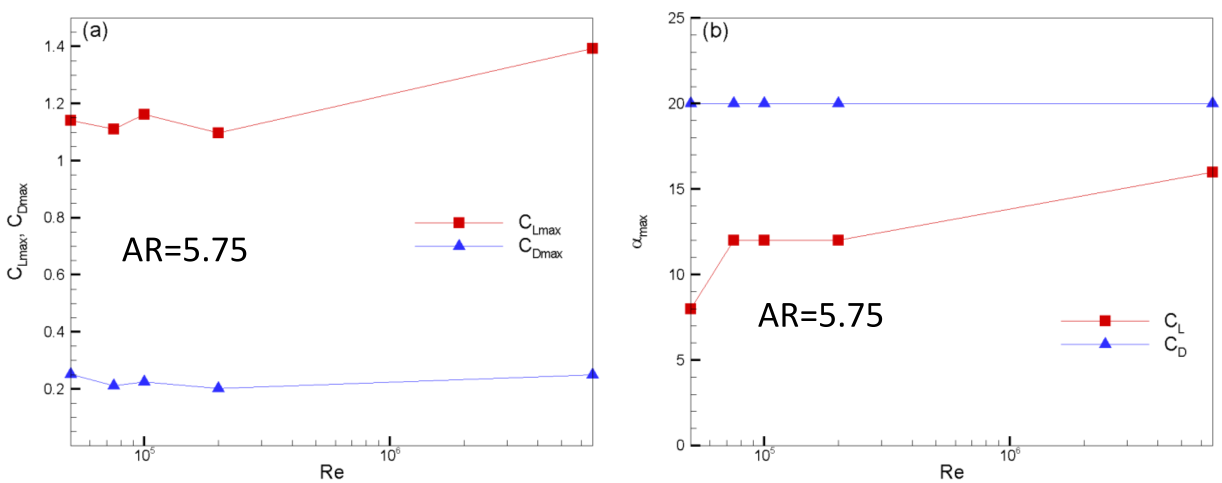

Fig. 4 Re dependency of C_{Lmax}, C_{Dmax} and α_{max} in Reference [2]: (a) C_{Lmax}, C_{Dmax} vs Re, (b) α_{max} vs Re

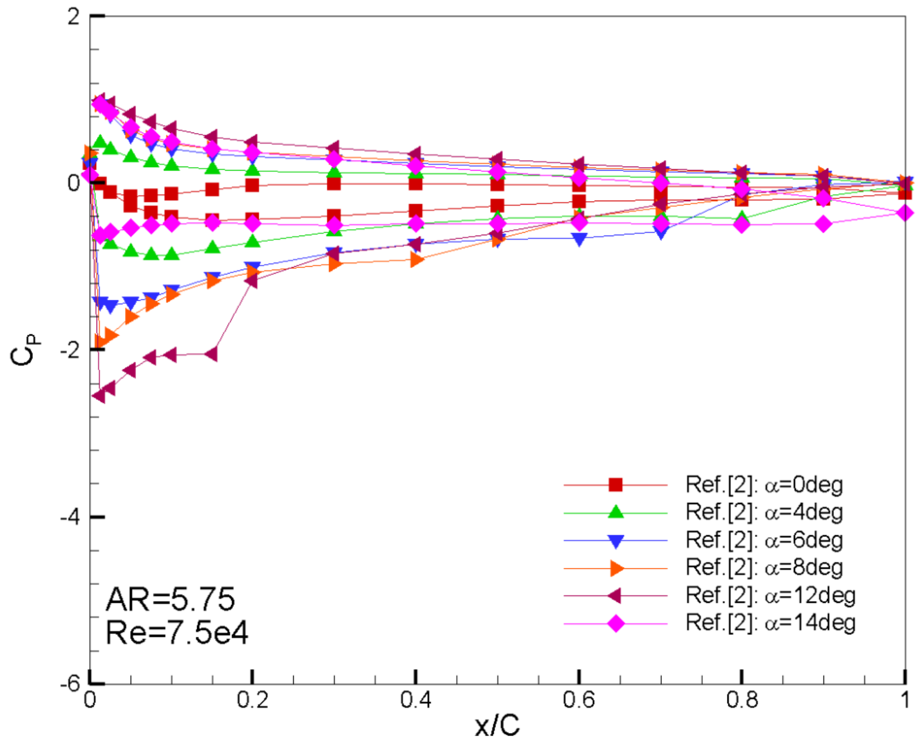

Fig. 5 Trend of C_P in Reference [2]

2.3 Reference [3]

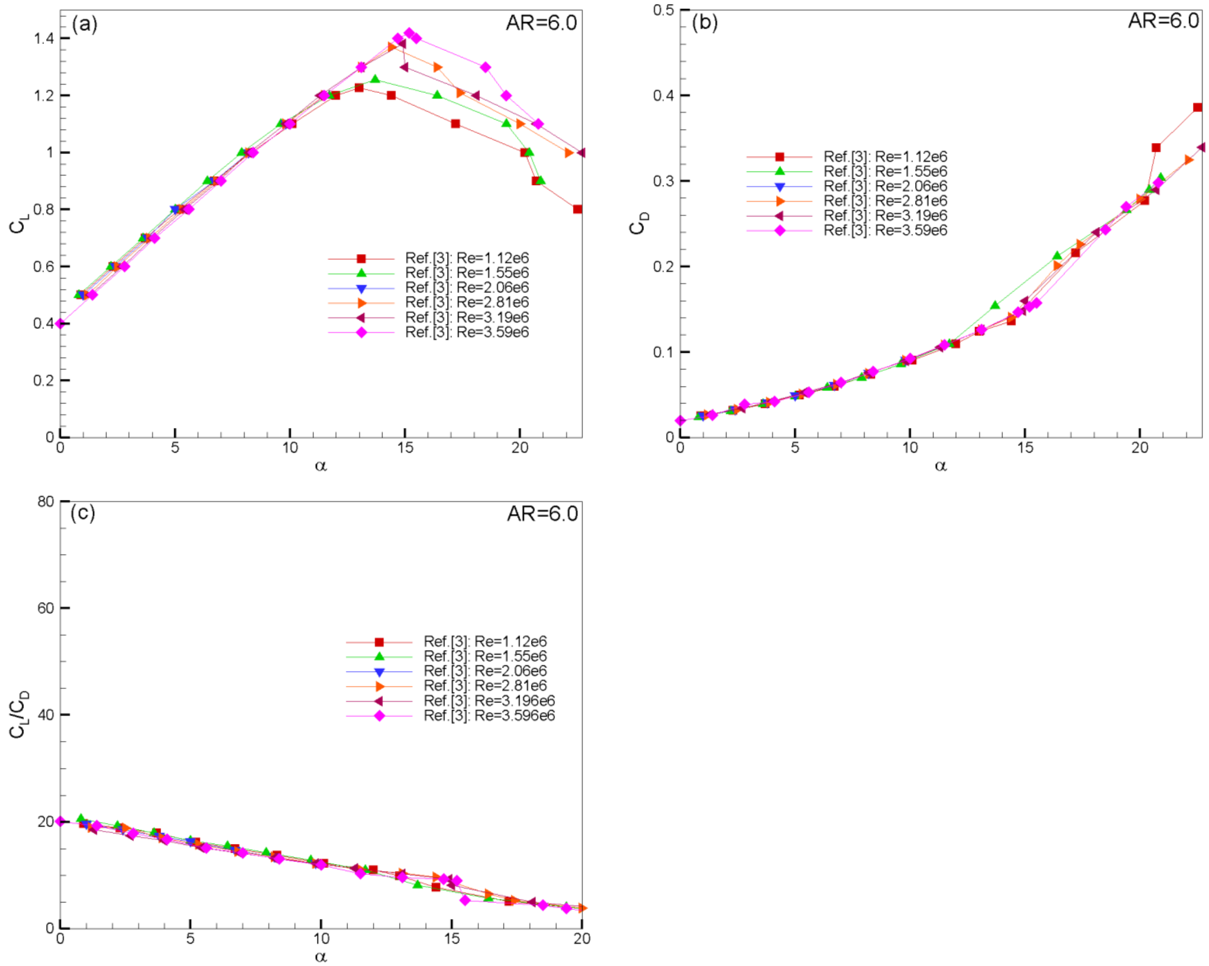

Fig. 6 Trend of C_L, C_D, and C_L/C_D with variations of Re in Reference [3]
(a) C_L vs α, (b) C_D vs α, (c) C_L/C_D vs α

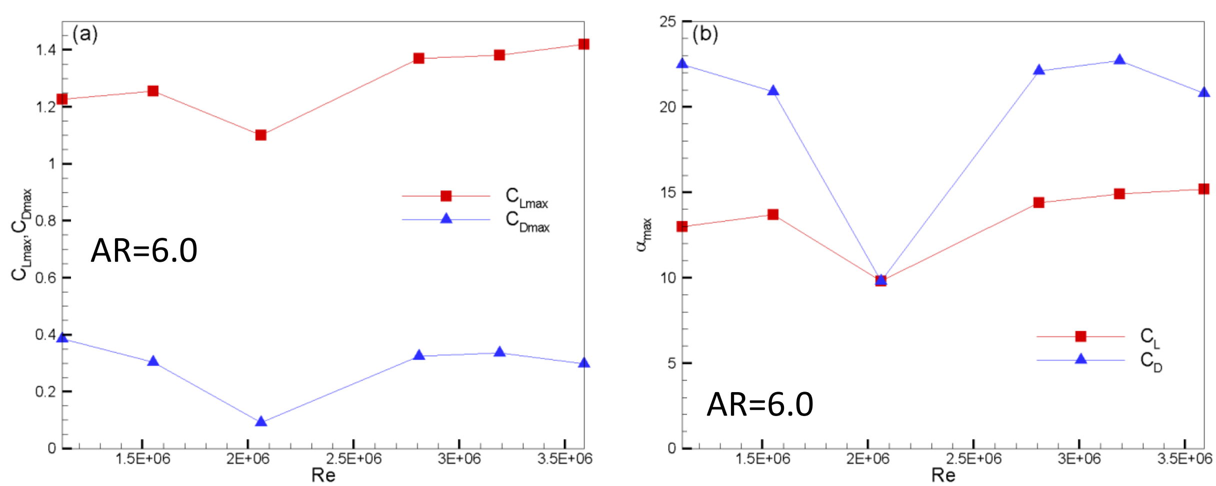

Fig. 7 Re dependency of C_{Lmax} and α_{max} for C_L in Reference [3]: (a) C_{Lmax} vs Re, (b) α_{max} vs Re

2.4 Reference [4]

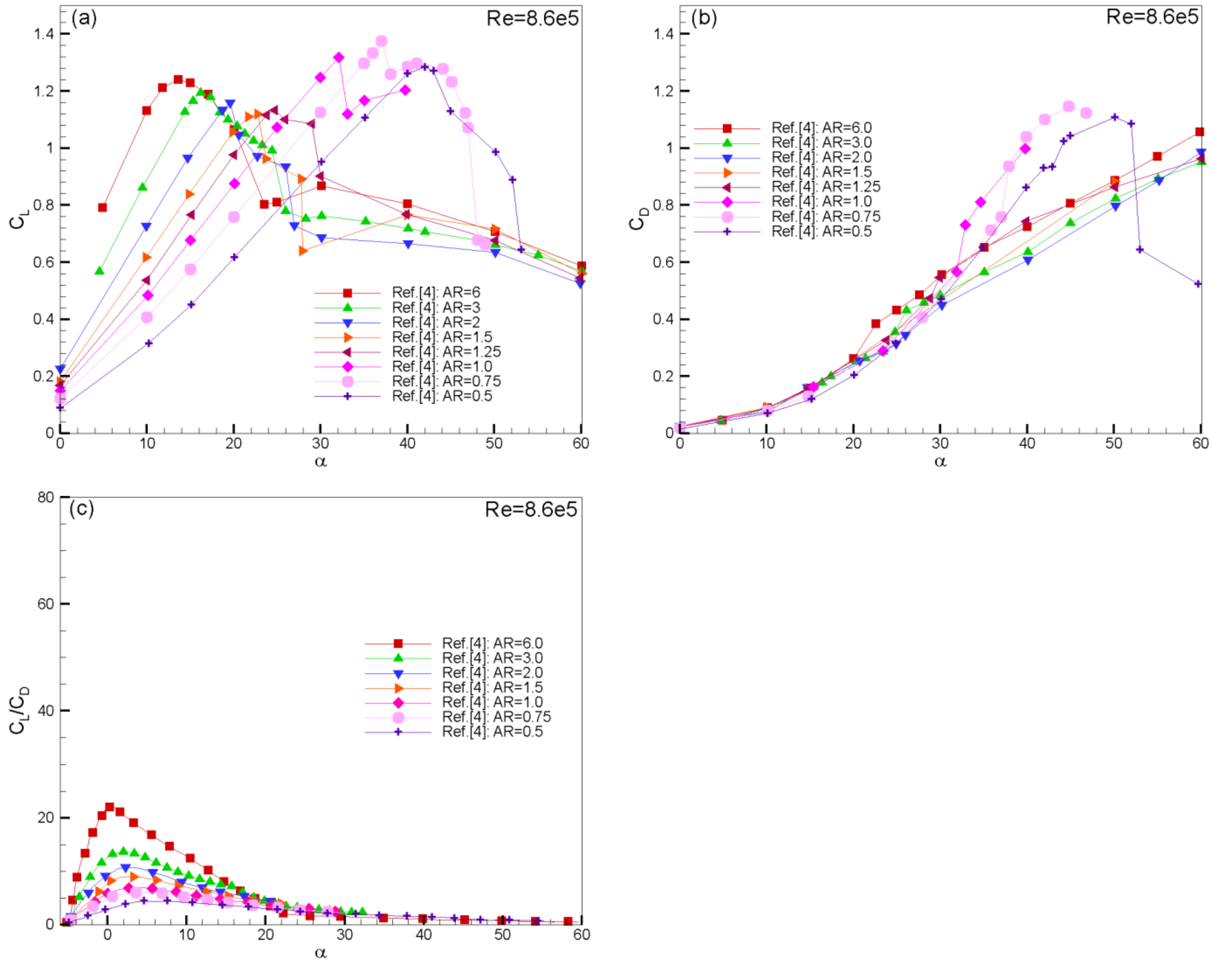

Fig. 8 Trend of C_L, C_D, and C_L/C_D with variations of AR in Reference [4]
(a) C_L vs α, (b) C_D vs α, (c) C_L/C_D vs α

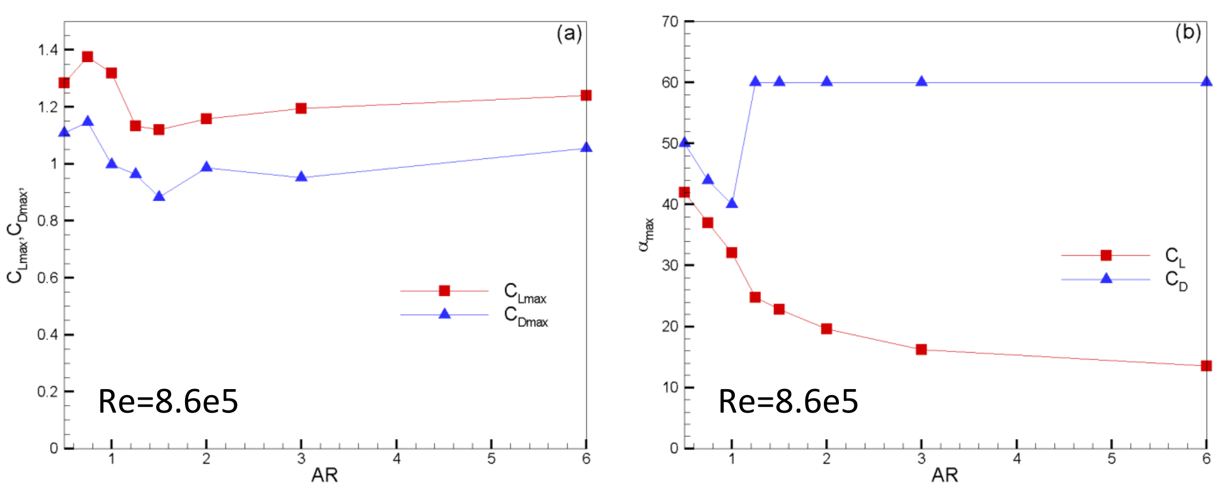

Fig. 9 Aspect ratio dependency of C_{Lmax} and α_{max} for C_L in Reference [4]: (a) C_{Lmax} vs AR, (b) α_{max} vs AR

3. Comparison between the reference experimental data

3.1 C_L vs α with largest AR

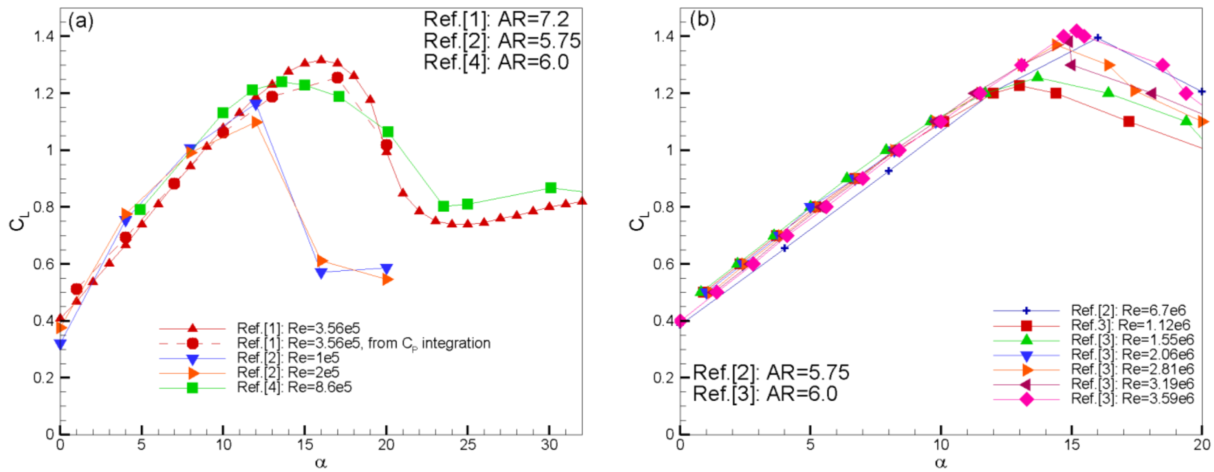

Fig. 10 C_L vs α with largest AR: (a) Re=O(10^5), (b) Re=O(10^6)

3.2 C_D vs α with largest AR

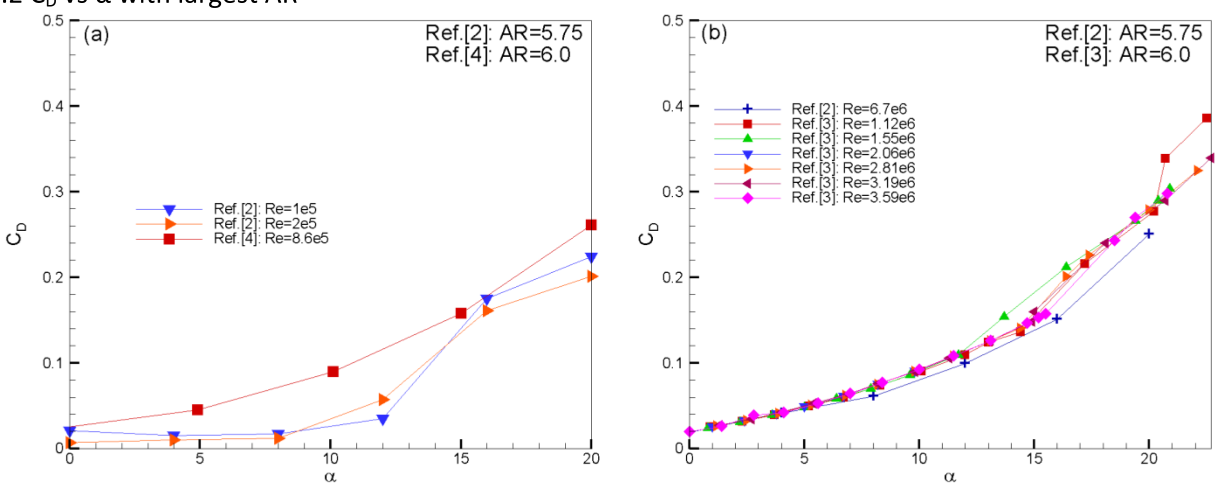

Fig. 11 C_D vs α with largest AR: (a) Re=O(10^5), (b) Re=O(10^6)

3.3 C_L/C_D vs α with largest AR

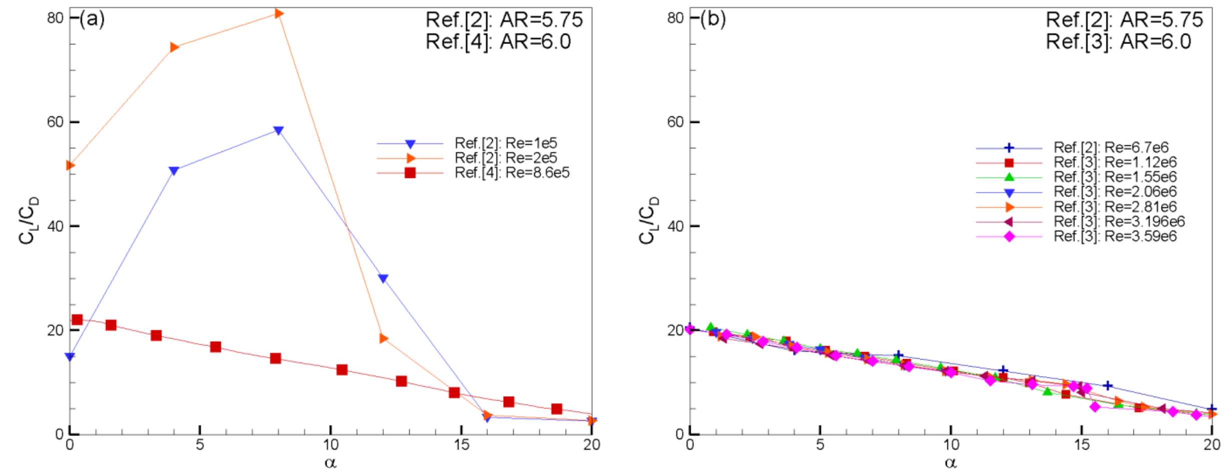

Fig. 12 C_D vs α with largest AR: (a) Re=O(10^5), (b) Re=O(10^6)

3.5 C_{Lmax}, C_{Dmax} and α_{max} with largest AR

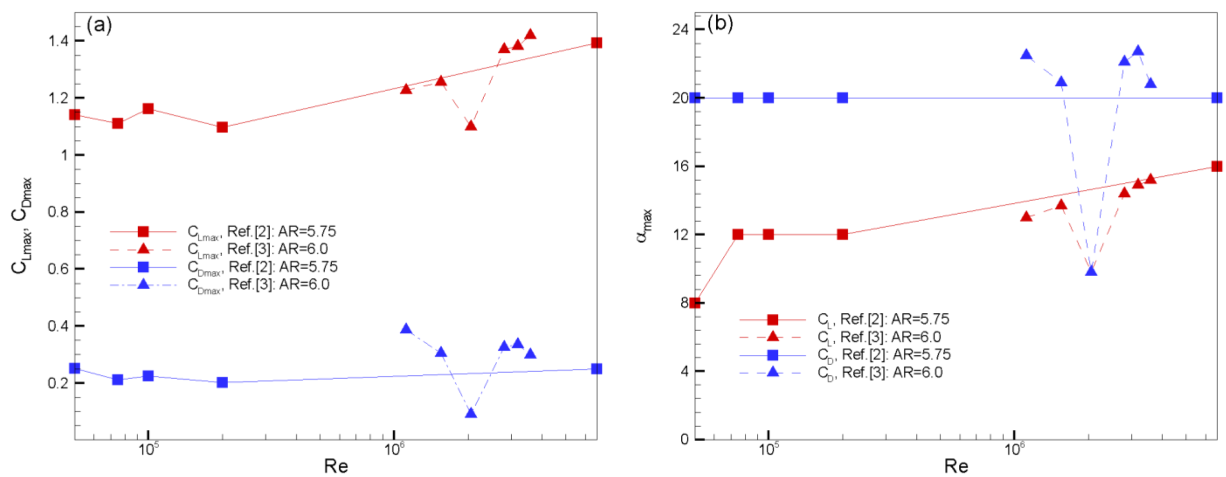

Fig. 13 Re dependency for C_{Lmax}, C_{Dmax} and α_{max}: (a) C_{Lmax}, C_{Dmax} vs Re, (b) α_{max} vs Re

3.4 C_P with largest AR

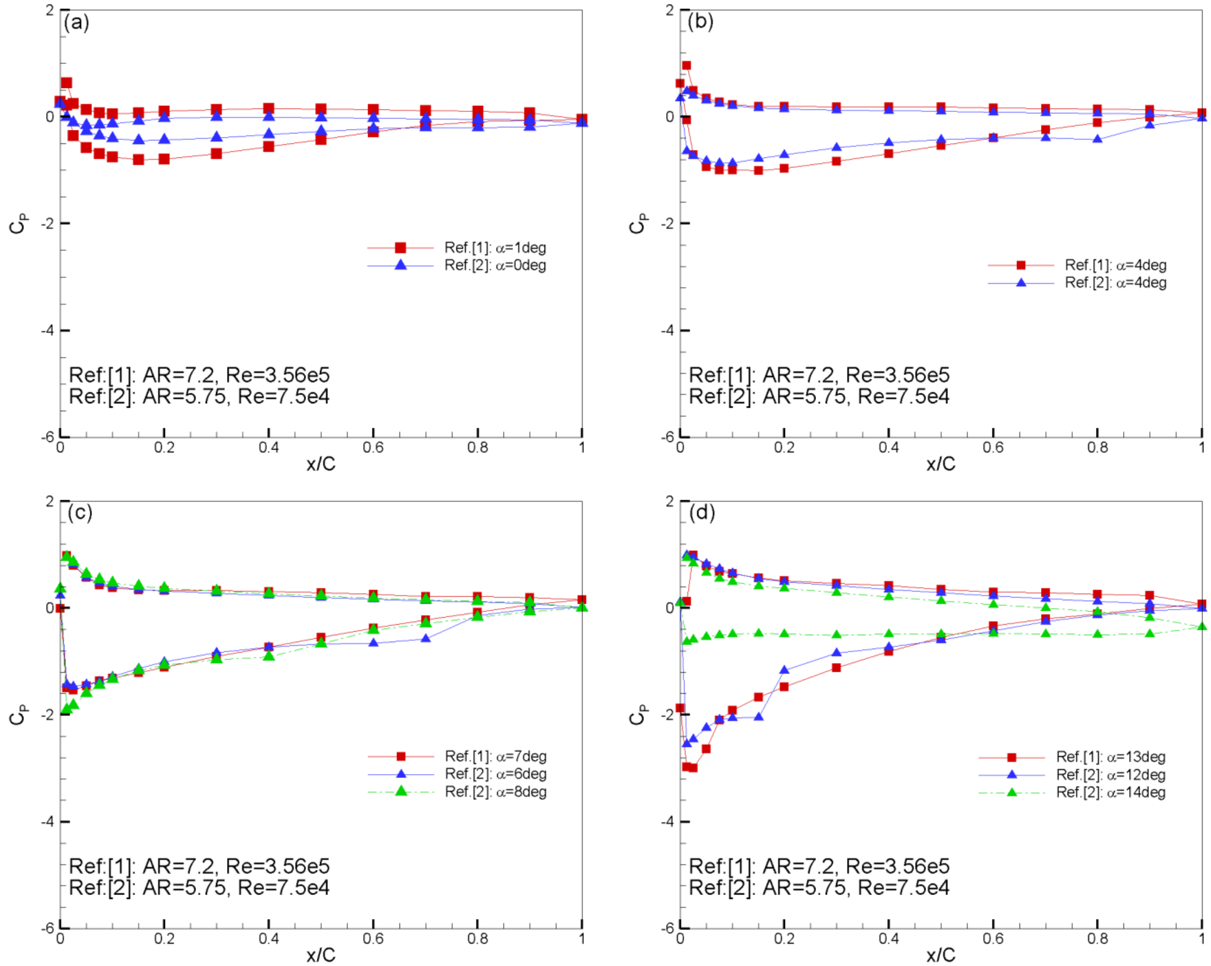

Fig. 14 C_P distribution with largest AR: (a) α≈0deg, (b) α≈4deg, (c) α≈7deg, (d) α≈13deg

4. Comparison with Flowlab simulation results

4.1 C_L vs α

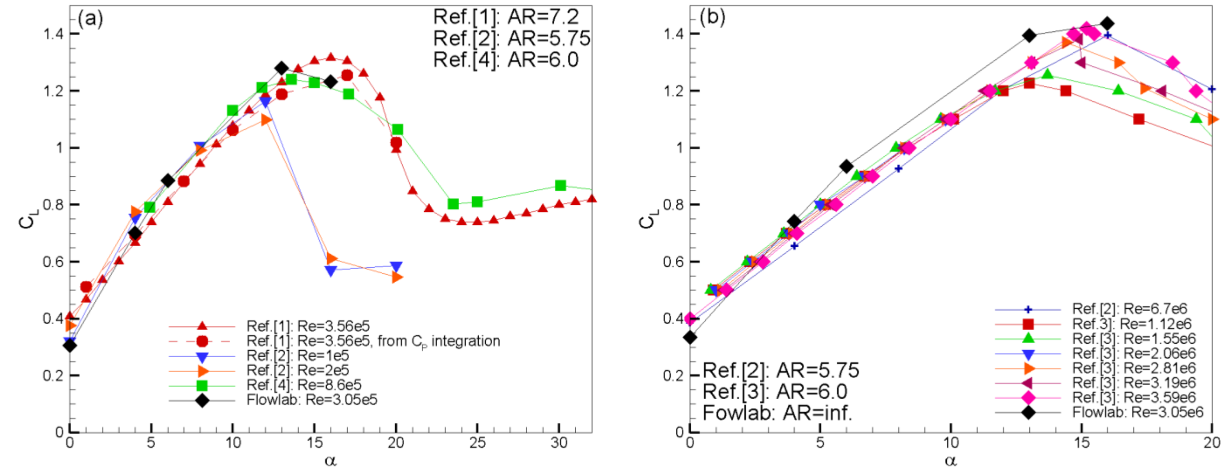

Fig. 15 C_L vs α with largest AR, Flowlab solutions added: (a) Re=O(10^5), (b) Re=O(10^6)

4.2 C_D vs α

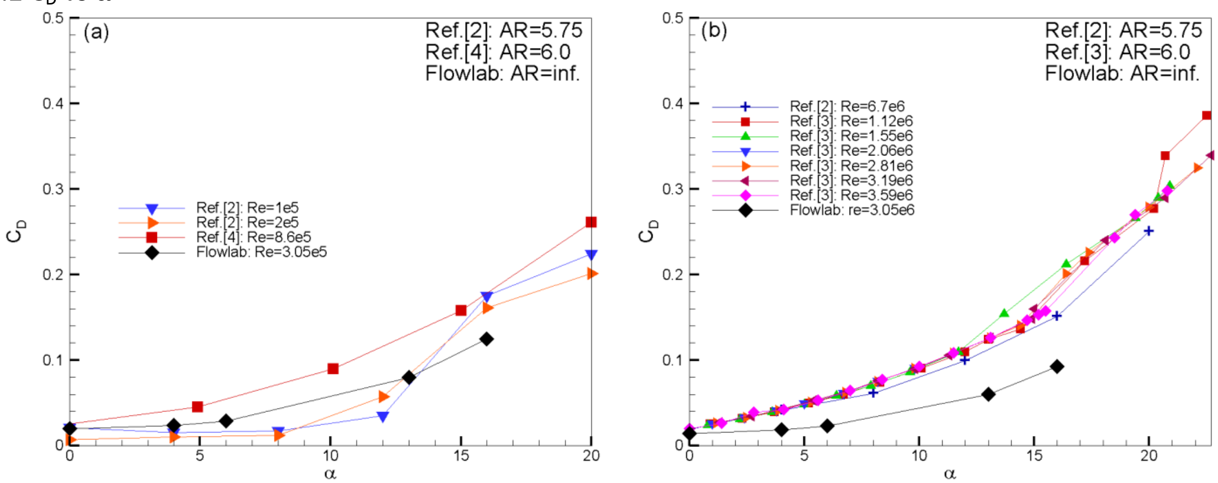

Fig. 16 C_D vs α with largest AR, Flowlab solutions added: (a) Re=O(10^5), (b) Re=O(10^6)

4.3 C_L/C_D vs α

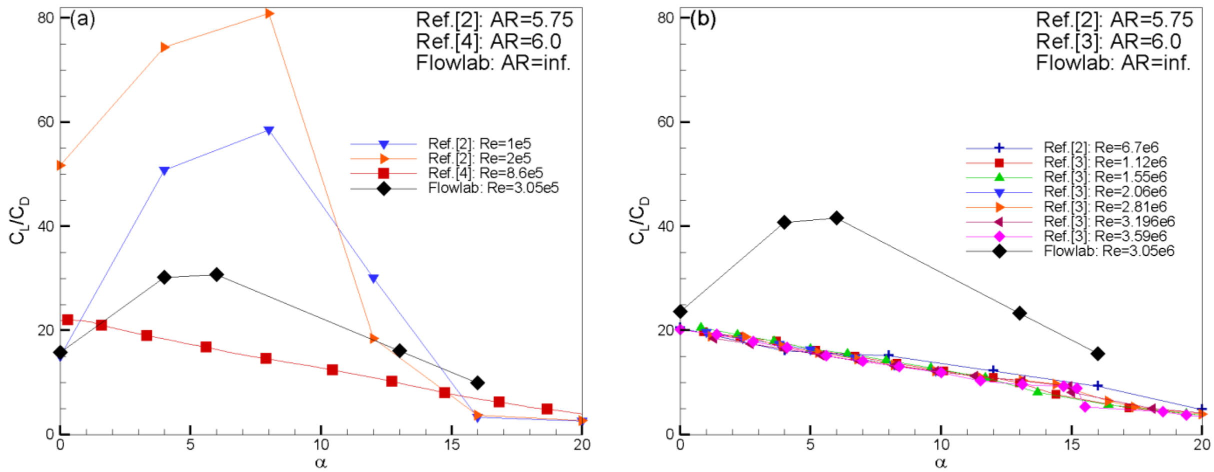

Fig. 17 C_D vs α with largest AR, Flowlab solutions added: (a) $Re=O(10^5)$, (b) $Re=O(10^6)$

4.3 C_P with largest AR

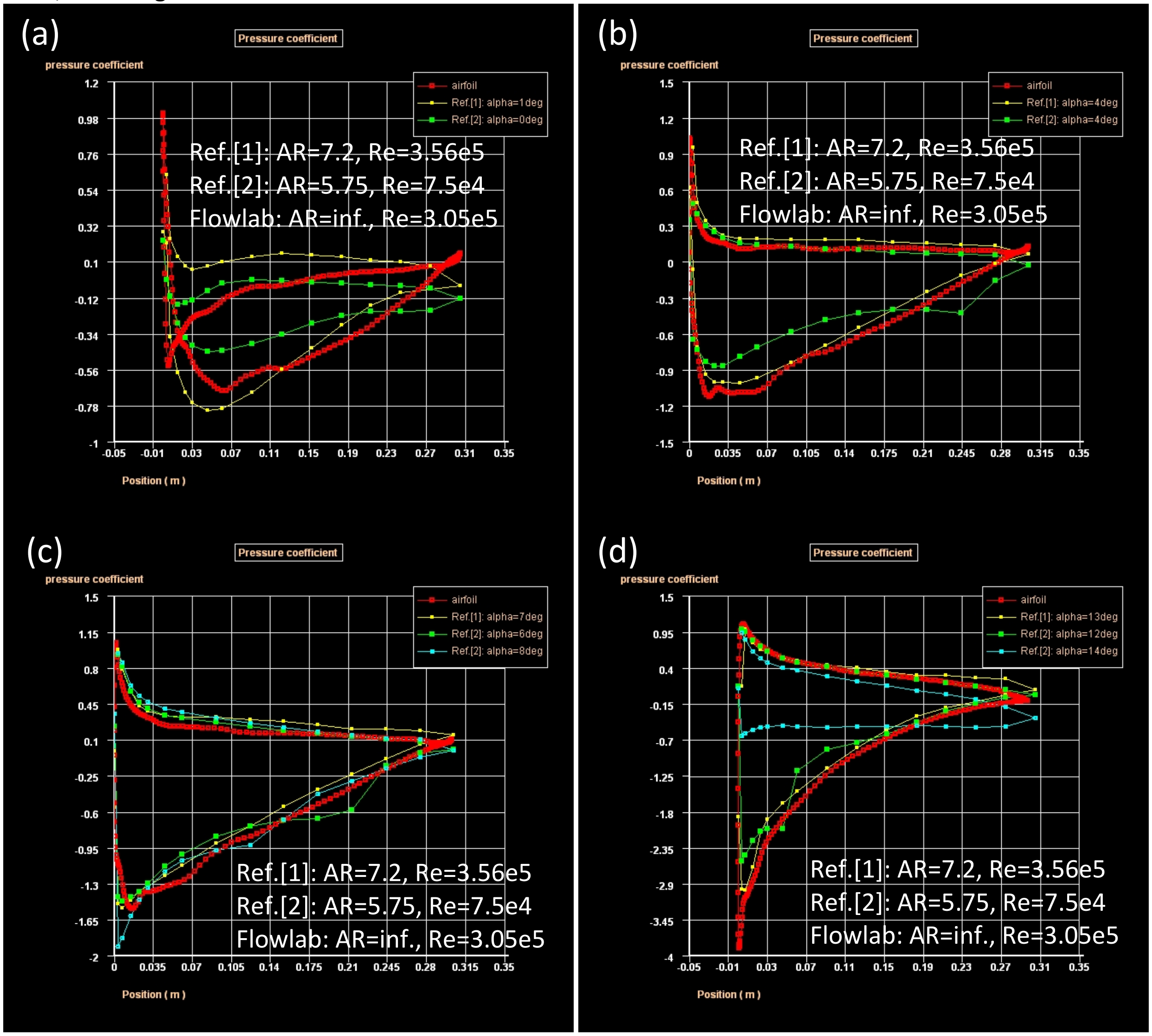

Fig. 18 C_P distribution with largest AR, Flowlab solutions added
(a) α≈0deg, (b) α≈4deg, (c) α≈7deg, (d) α≈13deg

5. Comparison between EFD benchmark data and IIHR experimental data

5.1 C_L vs α

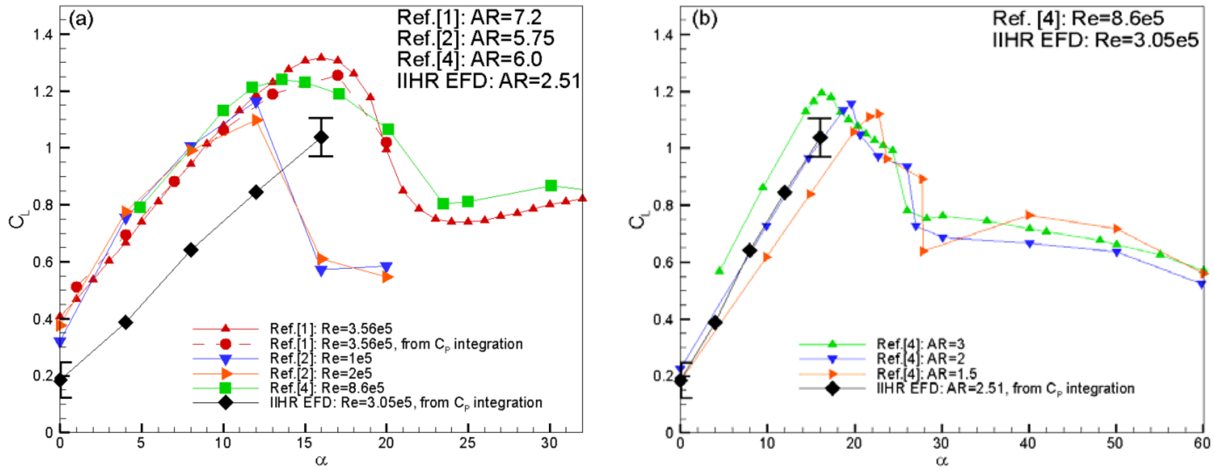

Fig. 19 C_L vs α, IIHR EFD data added: (a) large AR (≥5.75), (b) small AR (1.5≤AR≤3)

5.2 C_D vs α

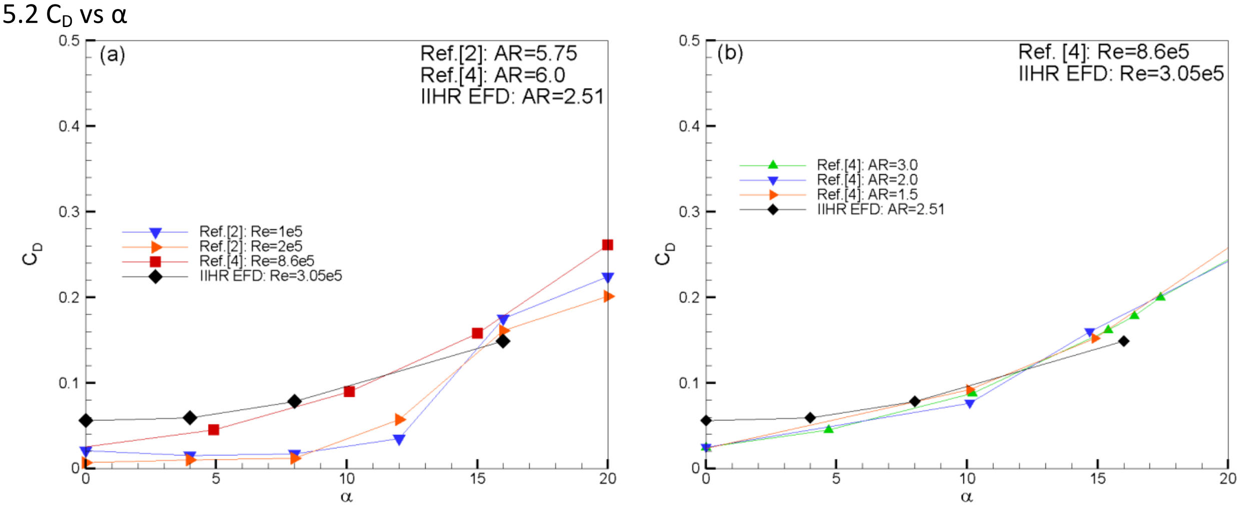

Fig. 20 C_D vs α, IIHR EFD data added: (a) large AR (≥5.75), (b) small AR (1.5≤AR≤3)

5.3 C_P

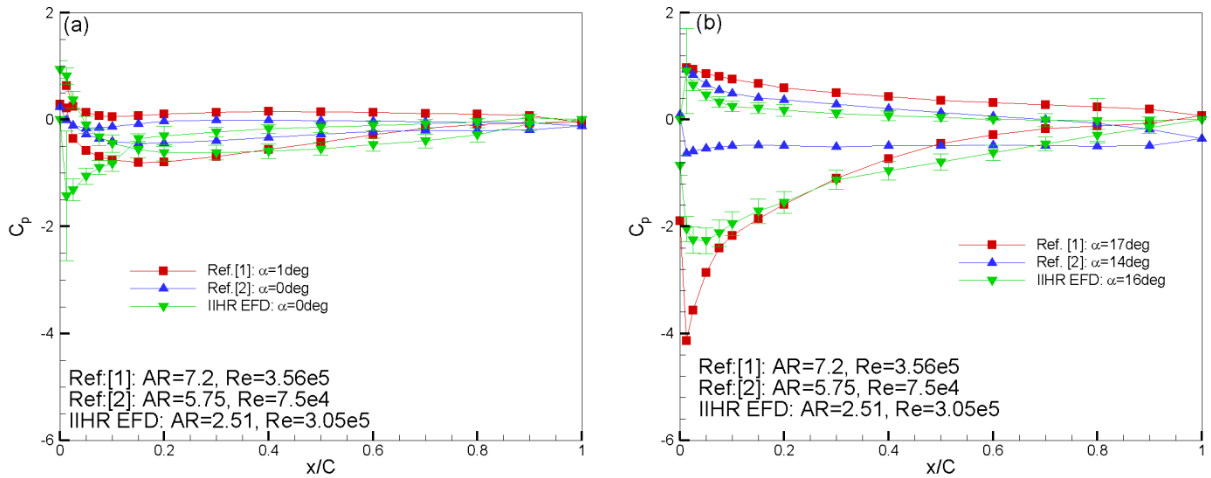

Fig. 21 C_P distribution, IIHR EFD data added: (a) α≈0deg, (b) α≈16deg

6. Comparison between EFD benchmark data, IIHR experimental data and Flowlab solution

6.1 C_L and C_D vs α

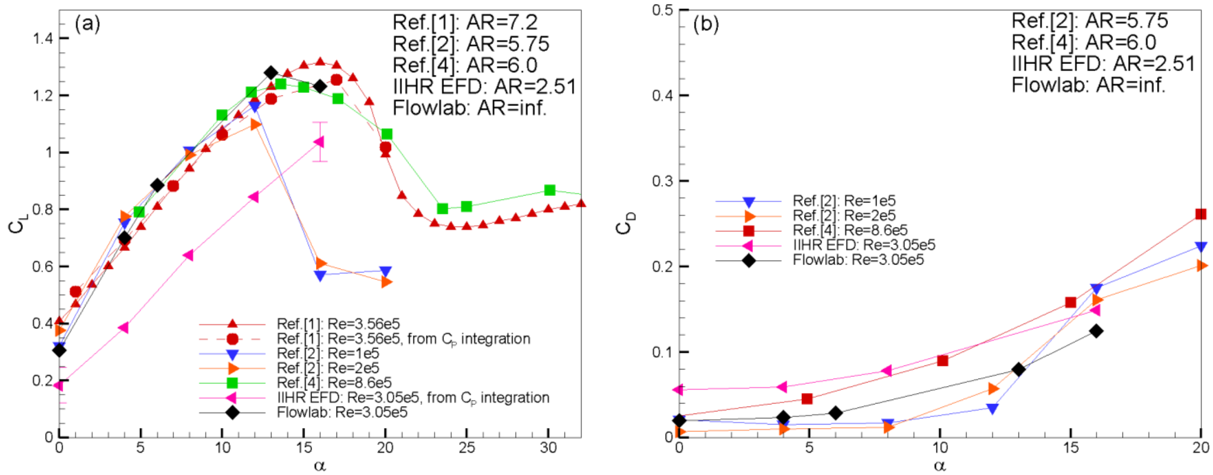

Fig. 22 C_L and C_D vs α: (a) C_L, (b) C_D

6.2 C_P

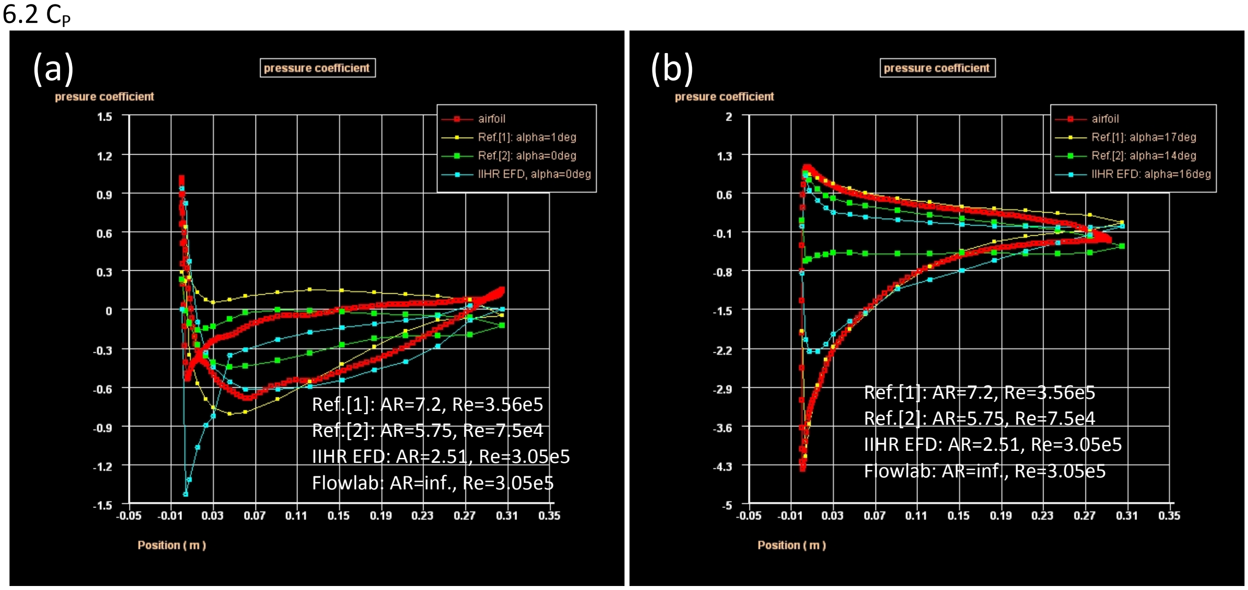

Fig. 23 C_P distribution: (a) α≈0deg, (b) α≈16deg

7. Discussion and Conclusion (To be added.)